29th International Cosmic Ray Conference Pune (2005) **10**, 213–226

Neutrino astronomy with IceCube and AMANDA

Gary Hill for the IceCube collaboration
Dept. of Physics, University of Wisconsin, Madison, WI 53706, USA
Presenter: Gary C. Hill (ghill@icecube.wisc.edu)

Since the early 1990's, the South Pole station in Antarctica has been the site of the development and operation of the world's first ice-Cherenkov neutrino telescopes, AMANDA and IceCube. The AMANDA telescope was completed in 2000 and has been used to search for the first high-energy neutrinos from beyond the earth. The successor to AMANDA, IceCube, will be a kilometre-scale neutrino and air shower detector with unprecedented sensitivity to astrophysical sources of neutrinos. In this paper, a summary of the results from AMANDA and report on the first construction season of the IceCube telescope will be given. The prospects for neutrino observation with the full IceCube array, slated for completion in 2010, will be discussed.

1. Introduction to high energy neutrino astronomy

The long-anticipated birth of experimental high-energy neutrino astronomy, pioneered by the DUMAND collaboration, has become a reality with the construction and operation of detectors such as AMANDA and Lake Baikal, the planned construction of other first-generation detectors, ANTARES, NESTOR and NEMO, and the initial construction of next generation detectors such as IceCube[1]. These instruments will look for signatures of high-energy neutrinos from some of the most energetic objects in the universe. The neutrino observations will complement and extend the understanding of the universe currently limited to cosmic-ray particle and photon observations.

Each of these three probes of the physics of the high-energy universe has its advantages and disadvantages as a messenger particle. Cosmic-ray particles (protons, neutrons and heavier nuclei) are readily detected at the earth, via space-borne particle detectors or via detectors of the extensive air showers that occur when these particles interact with the earth's atmosphere. However, due to the change in direction of these charged particles when propagating through magnetic fields during their travel to the earth, information about the source location is lost. The neutrons do of course trace the source direction but at lower energies they decay before reaching the earth and at the highest energies the sources are typically too far away for the neutrons to survive. There is one potential window for detection of galactic neutrons at 10^{18} eV. High-energy gamma rays will travel in straight lines and thus can point back to their source (as evidenced by the spectacular results from the new generation of Air-Cherenkov gamma-ray telescopes presented at this conference); however, there is reprocessing in sources and absorption of gamma rays from long distances across the universe, meaning that not all sources would be visible. For those sources that are visible, the nature of the acceleration mechanism is not known, with the potential origin usually suggested as either electromagnetic (synchrotron radiation of electrons, inverse Compton up-scattering of microwave photons) or hadronic (proton interactions producing pions that decay to gamma rays). High-energy neutrinos will propagate in straight lines unabsorbed, meaning that sources invisible at other wavelengths could be revealed; however, the low absorption makes them difficult to detect.

The neutrinos could solve the mystery of the origin of the cosmic rays. A typical high-energy cosmic accelerator is believed to consist of a compact object where the cosmic rays are accelerated. Some of these escape and eventually end up detected at earth. Some of these particles will interact both with themselves and with the radiation fields in the vicinity of the accelerator producing both charged and neutral pions. The neutral pions decay into high energy gamma rays and the charged pions decay into neutrinos. Thus, the coincident observa-

tion of neutrinos and gamma rays from the same source would be a clear indication of hadronic acceleration, suggesting such an observed source is a cosmic-ray accelerator.

Many predictions have been made for the expected rates of such high-energy neutrinos, both for individual objects and for the summed flux of all objects across the universe. Expectations of the existence of detectable fluxes led to the construction of the first purpose-built high-energy neutrino detectors, such as AMANDA, and now, to the construction of the next generation instruments, such as IceCube.

Construction of the AMANDA-II detector began in 1995[2] at the South Pole station, Antarctica and was completed in 2000, resulting in a detector consisting of 677 optical modules spread across 19 strings deployed at depths between 1500 and 2000 metres in the polar ice cap. The optical properties of the detector medium have been measured with in-situ light sources within the detector[3]. Most of the optical modules utilise analog signal technology, in which pulses are transmitted via electrical or fibre optic cable. A prototype digital string was deployed as part of the AMANDA detector[4] in order to test new technologies for IceCube.

Neutrinos are detected in several ways by a deep neutrino telescope such as AMANDA. All flavours of neutrino will produce hadronic cascades from charged and neutral current interactions within and close to the detection volume. The Cherenkov light from these cascades spreads in a known pattern away from the interaction vertex, and some of this light is detected by the optical modules, with the recorded times and amplitudes of the signals used to reconstruct the properties of the original neutrino.

Muon neutrinos may interact with the ice or rock far from the detector in a charged-current interaction, and the resulting muon may travel many kilometres to the detector where it is detected and reconstructed using the recorded information from its Cherenkov emissions.

Cosmic-ray interactions in the earth's atmosphere produce two types of background to a search for extra-terrestrial neutrinos – atmospheric muons and neutrinos. The atmospheric muons have a maximum range of the order of kilometres and thus are detected only from above the detector, those coming from below being absorbed by the earth. The atmospheric neutrinos will traverse the earth and be detected from all directions, although for the downward direction (zenith angles 0-90 degrees), their expected rate is swamped by the rate of the downward moving muons. Thus, the AMANDA detector looks down into the earth, seeking upward moving muons which can only have come from neutrino interactions, both atmospheric and extra-terrestrial in origin. The detection of an extra-terrestrial neutrino signal requires further rejection of the atmospheric neutrinos based on the the energies of the detected events.

The first evidence of high-energy atmospheric neutrinos in AMANDA came from the 1997 data set, where in the initial analysis, 16 candidate events remained after rejection of the downward moving atmospheric muon flux[5]. Further improvement of event selection techniques[6] led to the extraction of about 300 neutrino candidates from the 1997 data[7, 8].

Currently, utilising the four-year data set collected in 2000-03, several thousand atmospheric neutrinos have been detected[9]. As one tightens the event selection criteria, a clear separation of upward moving atmospheric neutrino induced muons can been seen from the more abundant flux of downward moving atmospheric muons[10], as shown in figure 1, where data is compared to expectations from Monte-carlo simulations of atmospheric neutrinos and muons. No evidence of a seasonal variation in the atmospheric neutrino flux has been seen[11].

The search for extra-terrestrial neutrinos and the study of potential cosmic-ray acceleration sites is just one topic of interest. Other interesting neutrino signatures are from exotic particles – e.g. WIMP annihilation in the centre of the earth and sun, topological defects, or low energy neutrinos from supernovae, detected via an increase in the noise rates of the sensors during a burst. A deep particle detector in conjunction with a surface air shower array can also study the composition of the cosmic rays around the knee of the spectrum.

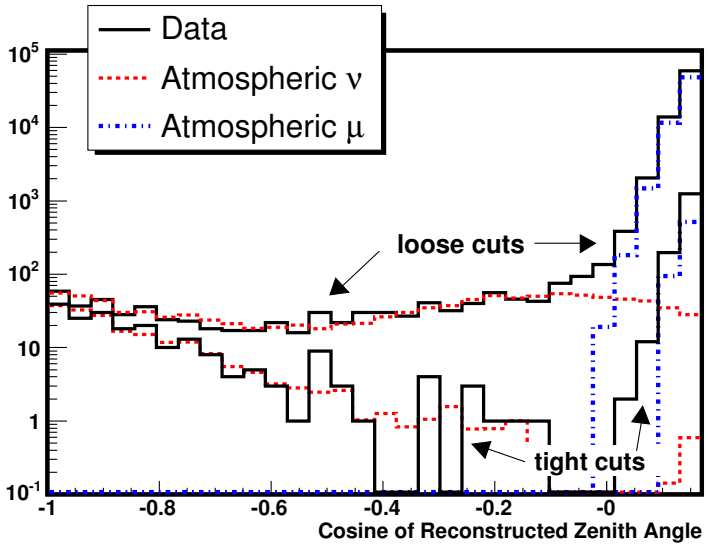

Figure 1. Atmospheric neutrinos and muons in AMANDA. As the quality selection of events is tightened, a clear separation is seen between the upward moving atmospheric neutrino-induced muons and the downward moving atmospheric muons.

Following in the footsteps of AMANDA, the kilometre-scale IceCube neutrino and air-shower detector is now under construction at the South Pole station in Antarctica. This detector will consist of a deep-ice component, 4800 optical sensors deployed across 80 strings at depths from 1400-2400 metres, and a surface component, the IceTop air shower array, consisting of 80 stations of 4 optical sensors deployed in ice tanks. The current IceCube collaboration consists of people from 28 institutions from across the USA (13), Europe (13), Japan, and New Zealand.

2. Results from AMANDA

The AMANDA data have produced many interesting physics results, and recent upgrades to the data acquisition system will further enhance the telescope capability. The main results and recent upgrades are summarised in this section.

2.1 Diffuse neutrinos

The AMANDA detector has been used in the search for diffuse neutrino fluxes via both muon and cascade detection methods, each with its unique advantages. Neutrino-induced muons that interact far outside the detector can be seen due to the long range of high-energy muons[10, 12], enhancing the effective detection volume. Cascade-like events[13, 14] from charged and neutral current interactions deposit most of their energy inside or close to the detector volume, allowing better primary neutrino energy determination. In both cases, the number of detector optical module channels (N_{ch}) registering at least one Cherenkov photon is used as an

Table 1. Summary of AMANDA diffuse neutrino flux results, 1997-2003. The results labelled "muon" are for analyses sensitive to neutrino-induced muon tracks in the detector, and give limits on the muon-neutrino flux at earth. The "all-flavour" analyses are sensitive to events from muon, electron and tau neutrinos, and place limits on the total neutrino flux at the earth, assuming a 1:1:1 flavour ratio due to maximal mixing neutrino oscillations during propagation to the earth. Assuming this 1:1:1 flavour ratio, the muon-neutrino limits may be converted to all-flavour limits by multiplying by three.

Data set	**Detection channel**	**Neutrino energy range TeV**	Limit $\mathrm{E}_\nu^2 \times \mathrm{dN}_\nu/\mathrm{dE}_\nu$(90%c.l.) $\mathrm{GeV\ cm^{-2}\ s^{-1}\ sr^{-1}}$	Reference
1997	muon	$6 - 10^3$	8.4×10^{-7}	[12]
1997	all flavour	$10^3 - 3 \times 10^6$	9.9×10^{-7}	[17]
1997	all flavour	$50 - 3 \times 10^3$	9.8×10^{-6}	[13]
2000	all flavour	$50 - 5 \times 10^3$	8.6×10^{-7}	[14]
2000	all flavour	$1.8 \times 10^2 - 1.8 \times 10^6$	$*3.8 \times 10^{-7}$	[16]
2000	muon, unfolding	$100 - 300$	2.6×10^{-7}	[15]
2000-03	muon	$16 - 2 \times 10^3$	$*1.1 \times 10^{-7}$	[10]
			* analysis in progress, sensitivity only	

energy estimator. Another technique is to "unfold" the neutrino spectrum[15], using a regularised unfolding technique. Since the number of unfolded events in the final energy spectrum does not follow Poisson statistics, a series of simulated data sets are constructed with various levels of signal contribution, then unfolded to determine probability distribution functions for the confidence interval construction. The muon detection channel analyses place limits of the muon-neutrino fluxes at the earth[12, 10, 15], while the cascade channel is used to place "all-flavour" limits on the total flux of muon-, electron- and tau-neutrino fluxes at the earth[13, 14, 16, 17] requiring an assumption on the flavour ratio, which is taken as 1:1:1, assuming that neutrinos are maximally mixed due to oscillations during their travel to the earth. Under the maximal mixing assumption, the muon-neutrino limits at earth can be converted to all-flavour limits by multiplying by three. The diffuse analyses are further divided into energy ranges. In the TeV-PeV energy range[17], extra-terrestrial neutrinos can traverse the earth and be detected. At higher energies, the earth becomes opaque to the neutrinos and thus the region around the horizon is examined for excesses of events above the atmospheric muon and neutrino expectations. Table 1 summarises the various diffuse analyses that have been performed with AMANDA data. For each, the type of analysis, sensitive energy range (90% of events), and limit on an E^{-2} flux is given.

The galactic plane is a potential source of high-energy neutrinos in the AMANDA detector, with the neutrino flux expected to result from the interaction of cosmic rays with the matter concentrated in the galactic plane. This search involves looking for an excess of events from a region extending a few degrees either side of the galactic plane. The sensitivity of AMANDA to detect galactic plane neutrinos was determined to be well above the predictions, and indeed this search found no significant excess of events, and limits were placed which were in line with the expected sensitivity[18].

2.2 Point source neutrinos

The northern sky has been searched for steady state and time variable point sources of neutrinos, using full-sky searches and searches for specific objects, usually based on observations in gamma rays or other wavelengths. Analyses performed on the 1997[19], 2000[20] and 2000-02[21] data sets have yielded no evidence for the existence of point sources of neutrinos. Recently, the four-year data set from 2000-03 has been analysed[9]. Figure 2 shows the sensitivity and neutrino effective area for the event selection, expected to be dominated by atmospheric neutrinos. The sky map of the northern sky, containing 3329 upgoing events, and distribution of significances are shown in figure 3. No evidence for the existence of a point source is seen. Limits are typically in the range $E_\nu^2 \times dN_\nu/dE_\nu = 6 \times 10^{-8}$ GeV cm^{-2} s^{-1}. Limits (integrated fluxes above 10 GeV) for specific sources are shown in table 2. The time-variability search[22] yielded no significant correlations of the neutrino events to any pre-determined objects. However, an a posteriori observation of three events in time correlation with the blazar 1ES 1959+650, while not statistically significant, has generated interest in the possibility of a future significant observation of such a correlation of neutrino observations with flary gamma-ray sources. In the regime between a completely diffuse search and individual point source search, there is the method of a stacking search, in which the observations from classes of object are summed. This search[23] found no significant excesses of events from a series of event classes.

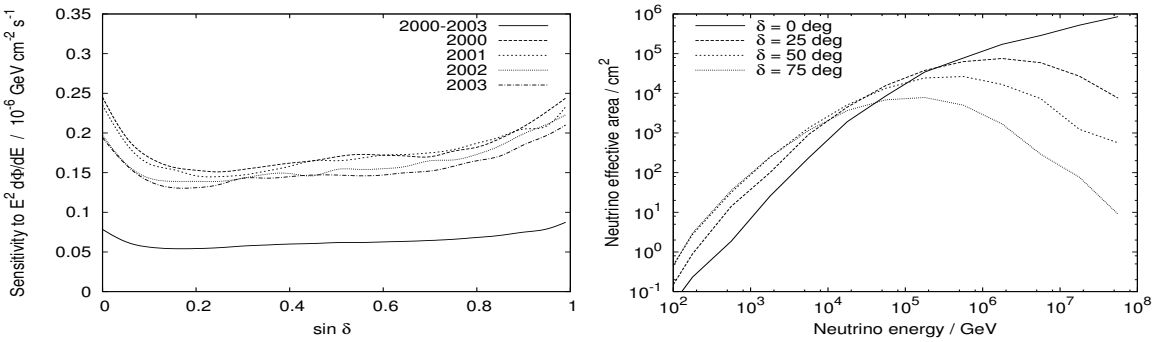

Figure 2. Left: Sensitivity of AMANDA-II as a function of declination (δ), for a signal spectral index of 2. The results for individual years and for the combined data sample are shown. Right: Neutrino effective area for AMANDA-II as a function of the neutrino energy.

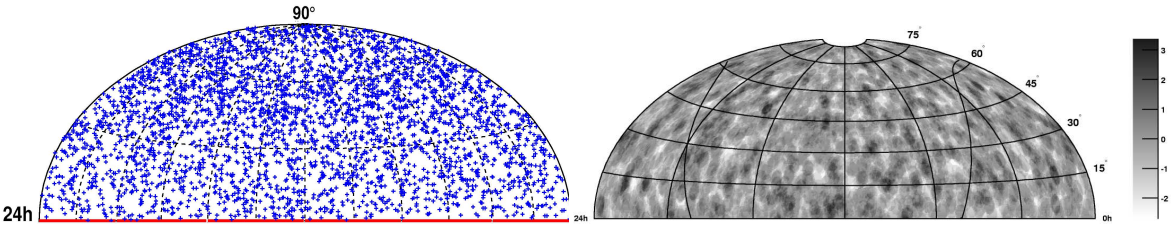

Figure 3. Left: Sky plot (in celestial coordinates) of the selected 3329 up-going neutrino candidate events observed in AMANDA-II. Right: Significance map from a scan of the northern sky to search for event clusters. The significance is positive for excesses and negative for deficits of events (compared to the expected background).

Table 2. Results from the AMANDA-II search for neutrinos from selected objects. δ is the declination in degrees, α the right ascension in hours, n_{obs} is the number of observed events, and n_b the expected background. $\Phi_\nu^{\rm lim}$ is the 90% CL upper limit in units of $10^{-8}{\rm cm}^{-2}{\rm s}^{-1}$ for a spectral index of 2 and integrated above 10 GeV. These results are preliminary (systematic errors are not included).

Candidate	$\delta(^\circ)$	α(h)	$n_{\rm obs}$	n_b	$\Phi_\nu^{\rm lim}$	Candidate	$\delta(^\circ)$	α(h)	$n_{\rm obs}$	n_b	$\Phi_\nu^{\rm lim}$
TeV Blazars											
Markarian 421	38.2	11.07	6	5.6	0.68	1ES 2344+514	51.7	23.78	3	4.9	0.38
Markarian 501	39.8	16.90	5	5.0	0.61	1ES 1959+650	65.1	20.00	5	3.7	1.0
1ES 1426+428	42.7	14.48	4	4.3	0.54						
GeV Blazars											
QSO 0528+134	13.4	5.52	4	5.0	0.39	QSO 0219+428	42.9	2.38	4	4.3	0.54
QSO 0235+164	16.6	2.62	6	5.0	0.70	QSO 0954+556	55.0	9.87	2	5.2	0.22
QSO 1611+343	34.4	16.24	5	5.2	0.56	QSO 0716+714	71.3	7.36	1	3.3	0.30
QSO 1633+382	38.2	16.59	4	5.6	0.37						
Microquasars											
SS433	5.0	19.20	2	4.5	0.21	Cygnus X3	41.0	20.54	6	5.0	0.77
GRS 1915+105	10.9	19.25	6	4.8	0.71	XTE J1118+480	48.0	11.30	2	5.4	0.20
GRO J0422+32	32.9	4.36	5	5.1	0.59	CI Cam	56.0	4.33	5	5.1	0.66
Cygnus X1	35.2	19.97	4	5.2	0.40	LS I +61 303	61.2	2.68	3	3.7	0.60
SNR & Pulsars											
SGR 1900+14	9.3	19.12	3	4.3	0.35	Crab Nebula	22.0	5.58	10	5.4	1.3
Geminga	17.9	6.57	3	5.2	0.29	Cassiopeia A	58.8	23.39	4	4.6	0.57
Miscellaneous											
3EG J0450+1105	11.4	4.82	6	4.7	0.72	J2032+4131	41.5	20.54	6	5.3	0.74
M 87	12.4	12.51	4	4.9	0.39	NGC 1275	41.5	3.33	4	5.3	0.41
UHE CR Doublet	20.4	1.28	3	5.1	0.30	UHE CR Triplet	56.9	11.32	6	4.7	0.95
AO 0535+26	26.3	5.65	5	5.0	0.57	PSR J0205+6449	64.8	2.09	1	3.7	0.24
PSR 1951+32	32.9	19.88	2	5.1	0.21						

2.3 Gamma-ray bursts

Gamma-ray bursts are amongst the most energetic objects in the universe. They have been routinely detected by satellite-borne detectors such as BATSE, HETE-II, and Swift. If these gamma-ray burst relativistic fireballs are also the site of hadron acceleration, then these objects could be the source of the highest energy cosmic rays[24]. Observation of neutrinos in coincidence with the bursts would confirm the hadronic acceleration. The search for neutrinos is straightforward – the satellite observation pinpoints the location in space and time of the burst, which is then searched for neutrino events in excess of expected backgrounds, which are accurately determined from the the on-source, off-time data. The expected number of events from a burst is determined from simulations of the detector response. Several types of search have been performed with AMANDA, utilising both muon and cascade data, and testing various models of gamma-ray production. The muon-neutrino searches utilise the full power of spatial and temporal rejection, whereas the cascades searches, despite the lack of directional information, make use of better event energy determination. One type of analysis assumes that the sum of all the GRBs produces a neutrino spectrum based on average burst parameters, as described by Waxman and Bahcall[25, 26]. In the other type of analysis, each burst is individually modelled based on experimental observation of gamma ray emission, red shift, etc., and the analyses individually tailored to the specific prediction[27]. Data coincident with gamma-ray bursts from 1997-2003 have been examined for neutrino emission and no excesses have been observed. Limits on the emission of neutrinos have been placed.

2.4 Searches for neutralino dark matter

Recent results from experimental cosmology suggest that about 23% of the universe is made up of non-baryonic cold dark matter. Minimally supersymmetric extensions to the Standard Model predict the existence of the neutralino, in the mass range GeV-TeV, which is a candidate for the cold dark matter. These relic neutralinos can become gravitationally trapped in the centres of objects like the earth and sun, where they annihilate pairwise and neutrinos are produced among the decays, which may then be detected in a high-energy neutrino detector. No excesses of events have been observed from the earth or sun and limits have been placed on the fluxes expected under various assumptions of neutralino mass and MSSM parameters[29, 30]. The AMANDA limits are competitive with those from other neutrino detectors, but the neutrino detector limits do not yet exclude the regions reached by the direct detection experiment, CDMS.

2.5 Searches for supernova neutrinos

The low-energy neutrinos detected from the supernova 1987A by the IMB and Kamiokande experiments heralded the birth of extra-solar neutrino astronomy. The AMANDA telescope, through monitoring of the count rates across the optical modules in the array, is sensitive to low-energy supernovae electron anti-neutrinos that interact within the detector volume, producing positrons that emit detectable light. An analysis of the data taken in 1997 and 1998 yielded a 90% confidence level upper limit of 4.3 supernovae in the galaxy[31]. AMANDA and IceCube are part of the world-wide SNEWS (Super Nova Early Warning System) network[32].

2.6 Cosmic ray composition

The combination of the SPASE air shower detector and the AMANDA detector provides a powerful tool for cosmic ray composition studies. The SPASE array measures the electron component of the air showers at the surface, and the AMANDA array measures the properties of the muons produced in the air showers. Together, these pieces of information provide a measurment of the mass composition of the cosmic rays around the knee of the spectrum. Analysis of the coincident SPASE-AMANDA data collected during 1998[33] indicates that the composition of the cosmic rays becomes heavier as the energy increases through the knee region.

2.7 New instumentation for the AMANDA data acquisition system

Completion of an upgrade to the AMANDA data acquisition system was accomplished in January 2003 with the addition of transient waveform recorders[34] to each of the optical sensor readouts, and a new triggering system[35] was added in January 2005. These TWRs record the complete shape of the pulse train arriving at the surface from the modules. Thus, the full information is available for analysis, in constrast to the standard muon DAQ which is based on time-to-digital (leading edge of pulses) and analog-to-digital converters (peak voltage of pulses). This system was limited to eight edges per optical module per triggered event and only one pulse height measurment. The addition of the TWR system should be particularly useful for bright events with many photons.

3. IceCube

The IceCube detector is under construction at the South Pole. IceCube will consist of two components – a kilometre-scale deep ice array of 4800 optical modules across 80 strings at depths from 1450 to 2450 metres and

a kilometre-scale surface air shower detector (IceTop), with 80 stations located at the surface above each string. Each IceTop station will contain four optical modules divided between two ice tanks. Each optical module consists of a ten-inch photomultiplier tube[36], which is read out by a recording device that digitises and time stamps the recorded waveforms before they are sent to the surface data acquisition system for processing. The DAQ assembles recorded waveforms into complete events, which are then reconstructed, filtered and transmitted via satellite to the collaboration for analysis. In this section we summarise the performance of the first instrumentation, the construction schedule, future technologies, and finally the expected performance of the full telescope.

3.1 First instrumentation and initial performance

The first instrumentation was deployed in 2004-05, with four IceTop stations and one deep-ice string now in operation. The IceTop stations were deployed early in the austral summer season, and the single deep-ice string was deployed in late January. After completion of the two-day hot water drilling of the hole, the complete deployment process – attachment of the 60 modules, lowering, and securing of the string at its final depth – took a total of 18 hours. Commissioning of the string included communications tests and initial performance tests of the modules, e.g. time calibration, noise rate checks and on-board LED flasher runs. Once the string and IceTop tanks were frozen in, more advanced tests were performed, in which atmospheric muons and air showers were reconstructed, both as separate detectors and in coincidence. The results compare favourably to expectations[37, 38].

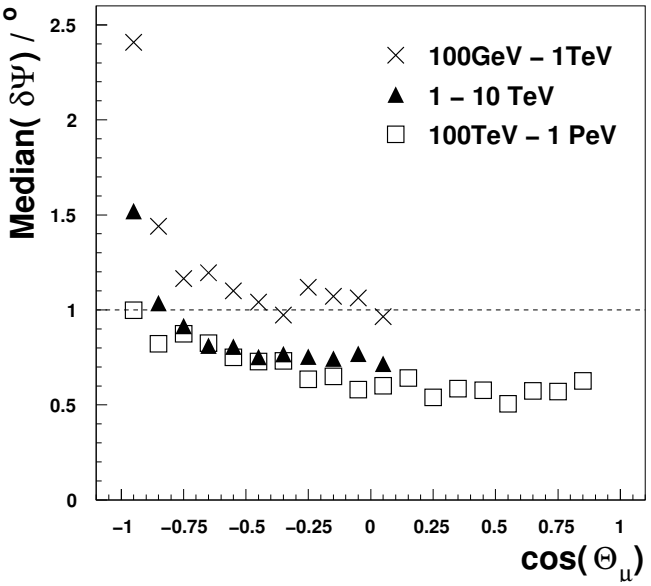

Figure 4. Pointing resolution for neutrino-induced muon events in IceCube. Shown is the median space angle error of the likelihood reconstruction as a function of the zenith angle of the incident track. The median was calculated for an energy spectrum $\propto E^{-2}$ and after applying level 2 cuts.

3.2 Construction schedule

Following the success of the first deployment season, the construction schedule calls for up to 12 strings to be deployed in 2005-06, followed by five more seasons of 16-18 strings, taking the detector to completion in early 2010. Physics data-taking will be routine during the construction cycle, and before completion, a square-kilometre-year exposure of data will have been accumulated.

3.3 Future development

The very highest energy neutrinos in the universe are expected to be produced when cosmic rays interact with the cosmic microwave background radiation. The planned IceCube detector would be able to detect of the order of one of these GZK neutrinos per year. Potential enhancements to the IceCube array could include the addition of radio and acoustic receivers on a grid expanding several kilometres away from the IceCube optical detector which would increase the number of detected GZK neutrinos by an order of magnitude[39].

3.4 Expected performance of the full IceCube telescope

The performance potential of IceCube has been estimated with a full simulation chain[40], based however on the AMANDA simulation packages. Both downward moving atmospheric muons and upward moving neutrino-induced muons were simulated and used to assess the capability of the detector to observe diffuse fluxes, point sources and gamma-ray bursts. The reconstruction methods were those from AMANDA[6], ignoring for now the full waveform information that IceCube will measure. A simple filtering scheme was implemented to reduce the atmospheric muons to a level at which only upward moving neutrino-induced muons should be seen (referred to as "level 2"). The angular pointing resolution is shown in figure 4. A median resolution of better than 1° is seen for events of energies greater than 1 TeV. The effective area for muon detection (figure 5) exceeds the geometric kilometre area for muon energies above 10 TeV and grows to 1.4 kilometre-squared for events from 1-100 PeV. From this point, the event selections were optimised for the best limit setting sensitivity[42] for each type of analysis.

Table 3. Sensitivity of IceCube to diffuse neutrino fluxes. Expected limits and minimal detectable fluxes in units of $\mathrm{GeV\ cm^{-2}\ s^{-1}\ sr^{-1}}$ for a generic E^{-2} source spectrum. Event numbers correspond to a hypothetical source strength of $E_\nu^2 \times dN_\nu/dE_\nu = 1 \times 10^{-7}\,\mathrm{GeV\ cm^{-2}\ s^{-1}\ sr^{-1}}$.

years	N_{ch} **Cut**	$\langle n_s \rangle$	$\langle n_b \rangle$	$\bar{\mu}_{90}$	$E^2 \frac{dN}{dE}(90\%\mathrm{c.l.})$	$E^2 \frac{dN}{dE}(5\sigma)$
1	227	76.4	8.0	6.1	$8.1 \cdot 10^{-9}$	$2.6 \cdot 10^{-8}$
3	244	204.8	18.4	8.7	$4.2 \cdot 10^{-9}$	$1.2 \cdot 10^{-8}$
5	276	272.5	18.0	8.6	$3.2 \cdot 10^{-9}$	$9.9 \cdot 10^{-9}$

For the case of a search for a diffuse flux following an E^{-2} spectrum, the distribution of the true neutrino energies are shown in figure 6 for the level 2 selection and after a cut on the number of channels ($\mathrm{N_{ch}}$)that recorded photons. The left-most plot shows the true energy distribution for the $\mathrm{E^{-2}}$ neutrino spectrum and shows that after the optimal cut at 227 fired channels; the detector is most sensitive to neutrinos at about 1 PeV. The right-most plot shows the same distribution of energies for the atmospheric neutrinos. There is also an as-yet-unknown background of atmospheric neutrinos from the decay of mesons containing charm quarks; all sensitivity calculation assume that this flux follows the RQPM prediction[41]. If the charm component is

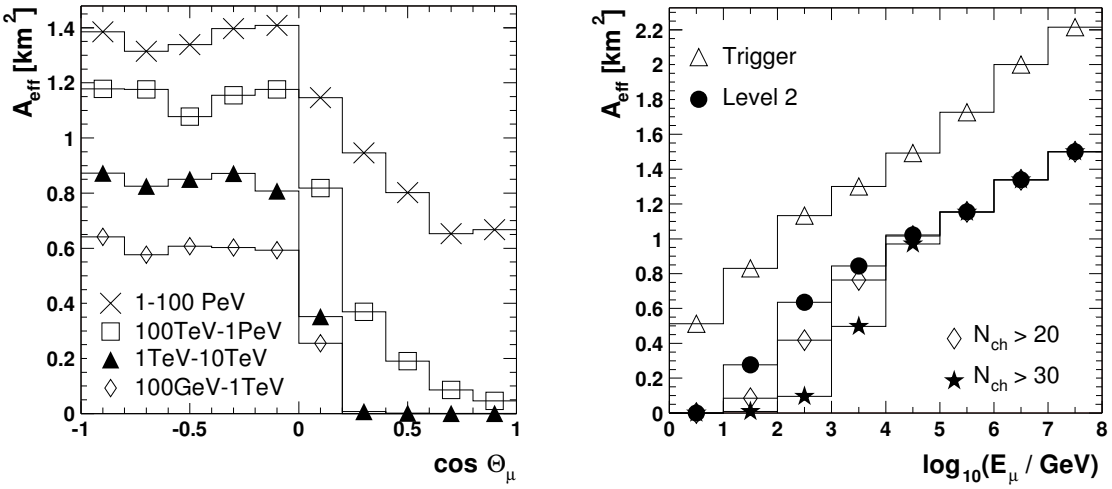

Figure 5. IceCube effective area as a function of the zenith angle after applying level 2 cuts (*left*) and as a function of the muon energy for different cut levels as described in the text (*right*). The zenith dependence is shown separately for different intervals of E_μ. The energy dependence holds for muons for which $\cos\Theta_\mu < 0$, *i.e.* muons that arrive from the northern sky. Energy cuts adjusted to signal spectra following E^{-2} and $E^{-2.5}$ power laws change the energy threshold.

less than this, the quoted sensitivities would improve, by up to more than a factor of two. Table 3 shows the expected sensitivity to an E^{-2} flux for various exposure times. For example, after three years of livetime, the optimal cut would be at 224 channels, where 18.4 background atmospheric neutrinos would remain. An E^{-2} flux of level corresponding to the present AMANDA-II four-year sensitivity would produce 204.8 events above this background and be readily observed. If only the background events were observed, the limit on the E^{-2} flux would be at a level of $\mathrm{E}_\nu^2 \times \mathrm{dN}_\nu/\mathrm{dE}_\nu = 4.2 \times 10^{-9}$ GeV cm^{-2} s^{-1}, about a factor 30 lower than the current AMANDA-II sensitivity. A true flux of strength one-tenth of the current limit sensitivity would be detectable at a 5σ level over the same three-year period.

Similar improvements in sensitivity over that of AMANDA-II are expected for point source searches, as summarised in table 4. The individual point source limits shown for AMANDA-II objects (table 2) are typically of the level 6×10^{-9} neutrinos cm^{-2}s^{-1}, integrated above 10 GeV. This corresponds to a limit on the normalisation of the differential E^{-2} flux of $\mathrm{E}_\nu^2 \times \mathrm{dN}_\nu/\mathrm{dE}_\nu = 6 \times 10^{-8}$ GeV cm^{-2} s^{-1}, which can be directly compared to the limiting and discovery fluxes in table 4. For three years of IceCube data taking, the limit is

Table 4. Sensitivity of IceCube to point sources of neutrinos. Expected limits and minimal detectable fluxes in units of GeV cm^{-2} s^{-1} for a generic E^{-2} source spectrum and different exposure times. Signal event rates correspond to a hypothetical source strength of $E_\nu^2 \times dN_\nu/dE_\nu = 1 \times 10^{-7}$ GeV cm^{-2} s^{-1}, background event rates include `rqpm` charm neutrinos.

years	N_{ch} **Cut**	$\langle n_s \rangle$	$\langle n_b \rangle$	$\bar{\mu}_{90}$	$E^2\frac{dN}{dE}(90\%c.l.)$	$E^2\frac{dN}{dE}(5\sigma)$
1	30	62.8	1.4	3.6	$5.5 \cdot 10^{-9}$	$1.7 \cdot 10^{-8}$
3	40	142.3	1.3	3.5	$2.4 \cdot 10^{-9}$	$7.2 \cdot 10^{-9}$
5	42	213.7	1.4	3.6	$1.7 \cdot 10^{-9}$	$4.9 \cdot 10^{-9}$

at $\mathrm{E}_\nu^2 \times \mathrm{dN}_\nu/\mathrm{dE}_\nu = 2.4 \times 10^{-9}$ GeV cm^{-2} s^{-1}, a factor 25 better than AMANDA-II, and a point source of strength about one-tenth of the AMANDA-II limit would be observed at a 5σ level of significance.

For the case of gamma-ray bursts, IceCube would need to observe only 100 satellite-coincident bursts to rule out the Waxman-Bahcall prediction at 90% confidence level, and observation of about 500 bursts would yield a 5σ observation if this flux were true.

It is also important to note that data will be taken with the IceCube detector (new strings plus the AMANDA array) during the construction phase, so that improving sensitivity will be seen as time passes – with an accumulated exposure of a square-kilometre-year, equivalent to the first line in the sensitivity tables (3 & 4) being reached before full completion.

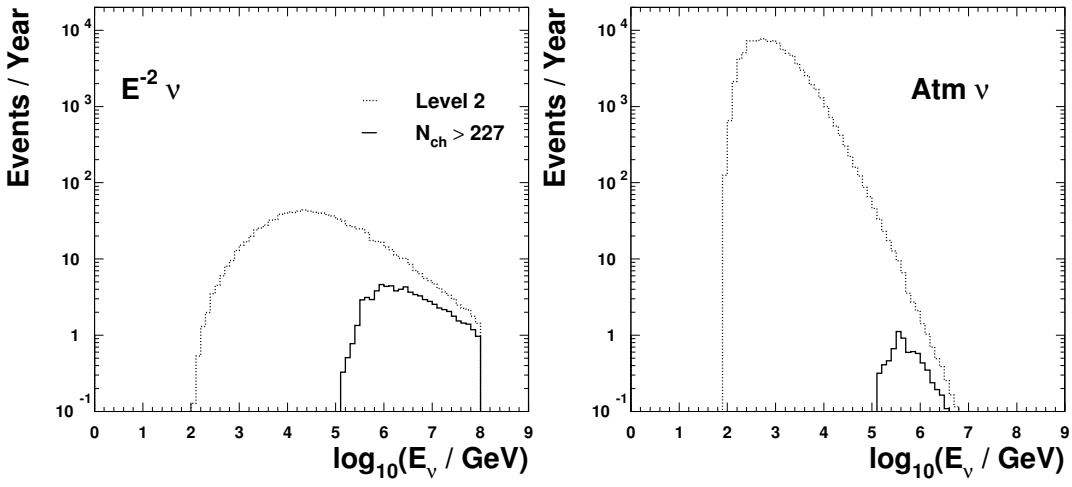

Figure 6. IceCube Energy spectra of selected neutrinos for a E^{-2} source (*left*) and atmospheric neutrinos (*right*). The selection is given by level 2 cuts (dotted lines) and application of the optimized cut $N_{\mathrm{ch}} > 227$ (full lines). The cutoff in the signal spectrum at 10^8 GeV is due to the limited energy range of simulation.

4. Conclusions

The last decade has seen the fruition of the first large ice and water Cherenkov neutrino detectors. The AMANDA telescope has been producing useful physics data since 1997 which has been examined for evidence of high-energy extra-terrestrial neutrinos, dark matter, and supernovae, and has also been used to measure cosmic ray properties. As yet, no sources of high energy neutrinos have been seen, however useful constraints on astrophysical models have been set. The IceCube detector, a kilometre scale detector also at the South Pole, will improve the sensitivity of current diffuse and point source searches by a factor of 30 and hopefully lead to many interesting and surprising discoveries about the nature of the universe.

5. Acknowledgements

GCH wishes to thank Tom Gaisser, Gaurang Yodh and Suresh Tonwar for providing the unexpected opportunity to present an AMANDA/IceCube highlight talk at the 29th ICRC in Pune.

The IceCube collaboration acknowledges the support of the following agencies: National Science Foundation–Office of Polar Programs, National Science Foundation–Physics Division, University of Wisconsin Alumni Research Foundation, Department of Energy, and National Energy Research Scientific Computing Center (supported by the Office of Energy Research of the Department of Energy), the NSF-supported TeraGrid systems at the San Diego Supercomputer Center (SDSC), and the National Center for Supercomputing Applications (NCSA); Swedish Research Council, Swedish Polar Research Secretariat, and Knut and Alice Wallenberg Foundation, Sweden; German Ministry for Education and Research, Deutsche Forschungsgemeinschaft (DFG), Germany; Fund for Scientific Research (FNRS-FWO), Flanders Institute to encourage scientific and technological research in industry (IWT), and Belgian Federal Office for Scientific, Technical and Cultural affairs (OSTC).

References

[1] For more information, see the IceCube website: http://icecube.wisc.edu
The complete set of 29th ICRC IceCube collaboration papers are available as one document at: http://arxiv.org/astro-ph/0509330

[2] E. Andres et al., *The AMANDA neutrino telescope: principle of operation and first results*, Astropart. Phys. 13 (2000) 1

[3] M. Ackermann et al., *Optical Properties of Deep Glacial Ice at the South Pole*, Journal of Geophysical Research, submitted (2005)

[4] M. Ackermann et al., *The ICECUBE prototype string in AMANDA*, Nuclear Inst. and Methods in Physics Research, A. accepted (2005)

[5] A. Karle for the AMANDA collaboration, *Observation of Atmospheric Neutrino Events with AMANDA*, Proceedings of the 26th International Cosmic Ray Conference, Salt Lake City, Utah (1999)

[6] J. Ahrens et al., *Muon track reconstruction and data selection techniques in AMANDA*, Nuclear Instruments and Methods in Physics Research A 524 (2004) 169

[7] J. Ahrens et al. (AMANDA Collaboration), *Observation of high energy atmospheric neutrinos with the Antarctic muon and neutrino detector array*, Phys. Rev. D 66, 012005 (2002)

[8] E. Andres et al., *Observations of High Energy Neutrinos with AMANDA*, Nature 410 441 (2001)

[9] M. Ackermann, E. Bernardini and T. Hauschildt for the IceCube Collaboration, *Search for high energy neutrino point sources in the northern hemisphere with the AMANDA-II neutrino telescope*, Proc. 29th ICRC, Pune, 5, 5 (2005).

[10] J. Hodges for the IceCube Collaboration, *Search for Diffuse Flux of Extraterrestrial Muon Neutrinos using AMANDA-II Data from 2000 to 2003*, Proc. 29th ICRC, Pune, 5, 115 (2005). The presented limit sensitivity ($E_\nu^2 \times dN_\nu/dE_\nu = 1.1 \times 10^{-7} \mathrm{GeV\ cm^{-2}\ s^{-1}\ sr^{-1}}$) was an update over that quoted in the proceedings ($E_\nu^2 \times dN_\nu/dE_\nu = 0.95 \times 10^{-7} \mathrm{GeV\ cm^{-2}\ s^{-1}\ sr^{-1}}$).

[11] M. Ackermann and E. Bernardini for the IceCube Collaboration, *An investigation of seasonal variations in the atmospheric neutrino rate with the AMANDA-II neutrino telescope*, Proc. 29th ICRC, Pune, 9, 107 (2005).

[12] J. Ahrens et al., *Limits on Diffuse Fluxes of High Energy Extraterrestrial Neutrinos with the AMANDA-B10 Detector*, Phys. Rev. Lett. 90, 251101 (2003)

[13] J. Ahrens et al. (AMANDA Collaboration), *Search for neutrino-induced cascades with the AMANDA detector*, Phys. Rev. D 67, 012003 (2003)
[14] M. Ackermann et al., *Search for neutrino-induced cascades with AMANDA*, Astropart. Phys. 22 127 (2004)
[15] K. Münich for the IceCube Collaboration, *Search for a diffuse flux of non-terrestrial muon neutrinos with the AMANDA detector*, Proc. 29th ICRC, Pune, 5, 17 (2005).
[16] L. Gerhardt for the IceCube Collaboration, *Sensitivity of AMANDA-II to UHE Neutrinos*, Proc. 29th ICRC, Pune, 5, 111 (2005).
[17] M. Ackermann et al., *Flux limits on ultra high energy neutrinos with AMANDA-B10*, Astropart. Phys. 22 339 (2005)
[18] J. L. Kelley for the IceCube Collaboration, *A Search for High-energy Muon Neutrinos from the Galactic Plane with AMANDA-II*, Proc. 29th ICRC, Pune, 5, 127 (2005).
[19] J. Ahrens et al, *Search for Point Sources of High Energy Neutrinos with AMANDA*, Astrophys. J 583 1040 (2003)
[20] J. Ahrens et al., *Search for Extraterrestrial Point Sources of Neutrinos with AMANDA-II*, Phys. Rev. Lett. 92, 071102 (2004)
[21] M. Ackermann et al., *Search for extraterrestrial point sources of high energy neutrinos with AMANDA-II using data collected in 20002002*, Phys. Rev. D 71, 077102 (2005)
[22] M. Ackermann, E. Bernardini, T. Hauschildt and E. Resconi, *Multiwavelength comparison of selected neutrino point source candidates*, Proc. 29th ICRC, Pune, 5, 1 (2005).
[23] A. Groß and T. Messarius for the IceCube Collaboration, *A source stacking analysis of AGN as neutrino point source candidates with AMANDA*, Proc. 29th ICRC, Pune, 5, 13 (2005).
[24] E. Waxman and J. Bahcall, *High Energy Neutrinos from Cosmological Gamma-Ray Burst Fireballs*, Phys. Rev. Lett. 78, 2292-2295 (1997)
[25] K. Kuehn for the IceCube Collaboration and the IPN Collaboration, *The Search for Neutrinos from Gamma-Ray Bursts with AMANDA*, Proc. 29th ICRC, Pune, 5, 131 (2005).
[26] B. Hughey, I. Taboada for the IceCube Collaboration, *Neutrino-Induced Cascades From GRBs With AMANDA-II*, Proc. 29th ICRC, Pune, 5, 119 (2005).
[27] M. Stamatikos, J. Kurtzweil and M. J. Clarke for the IceCube Collaboration, *Probing for Leptonic Signatures from GRB030329 with AMANDA-II*, Proc. 29th ICRC, Pune, 4, 471 (2005).
[28] J. Ahrens et al. (AMANDA Collaboration), *Limits to the muon flux from WIMP annihilation in the center of the Earth with the AMANDA detector*, Phys. Rev. D 66, 032006 (2002)
[29] D. Hubert, A. Davour, C. de los Heros for the IceCube Collaboration, *Search for neutralino dark matter with the AMANDA neutrino detector*, Proc. 29th ICRC, Pune, 9, 179 (2005).
[30] A. Achterberg et al., *Limits to the muon flux from neutralino annihilations in the Sun with the AMANDA detector*, Astropart. Phys. accepted for publication (2005)
[31] J. Ahrens et al., *Search for supernova neutrino bursts with the AMANDA detector*, Astropart. Phys. 16 (2002) 345
[32] SNEWS: The SuperNova Early Warning System, http://snews.bnl.gov/
[33] J. Ahrens et al. (AMANDA and SPASE Collaborations), *Measurement of the cosmic ray composition at the knee with the SPASE-2/AMANDA-B10 detectors*, Astropart. Phys. 21 (2004) 565
[34] A. Silvestri for the IceCube Collaboration, *Performance of AMANDA-II using Transient Waveform Recorders*, Proc. 29th ICRC, Pune, 5, 431 (2005).
[35] T. Messarius for the IceCube Collaboration, *A software trigger for the AMANDA neutrino detector*, Proc. 29th ICRC, Pune, 5, 207 (2005).
[36] H. Miyamoto for the IceCube Collaboration, *Calibration and characterization of photomultiplier tubes of the IceCube neutrino detector*, Proc. 29th ICRC, Pune, 5, 63 (2005).

[37] D. Chirkin for the IceCube Collaboration, *IceCube: Initial Performance*, Proc. 29th ICRC, Pune, 8, 303 (2005).
[38] T. K. Gaisser for the IceCube Collaboration, *Air showers with IceCube: First Engineering Data*, Proc. 29th ICRC, Pune, 8, 315 (2005).these proceedings
[39] J. A. Vandenbroucke for the IceCube Collaboration, *Simulation of a Hybrid Optical/Radio/Acoustic Extension to IceCube for EeV Neutrino Detection*, Proc. 29th ICRC, Pune, 5, 21 (2005).
[40] J. Ahrens et al. (IceCube collaboration), *Sensitivity of the IceCube detector to astrophysical sources of high energy muon neutrinos*, Astropart. Phys. 20 (2004) 507
[41] E.V. Bugaev et al., Phys. Rev. D 58 (1998) 054001
[42] G.C. Hill & K. Rawlins, *Unbiased cut selection for optimal upper limits in neutrino detectors: the model rejection potential technique*, Astropart. Phys. 19 (2003) 393